Published in: Geophysical Research Letters (2003), vol. 30, iss. 18
Status: Postprint (Author's version)

High resolution FUV observations of proton aurora

D. H. Chua,[1] K. F. Dymond,[1] S. A. Budzien,[1] R. P. McCoy,[2] J.-C. Gérard,[3] V. Coumans,[3] D. Bisrkalo,[4] and V. Shematovich[4]

[1]*Thermospheric and Ionospheric Research and Applications Group, Naval Research Laboratory, Washington, DC, USA.*
[2]*Office of Naval Research, Arlington, Virginia, USA.*
[3]*Laboratoire de Physique Atmosphèrique et Planétaire, Université de Liège, Liège, Belgium.*
[4]*Institute of Astronomy, Russian Academy of Sciences, Moscow, Russia.*

[1] We present new FUV observations of Doppler-shifted Lyman-α emissions from proton aurora obtained from the High Resolution Ionospheric and Thermospheric Spectrograph (HITS) aboard the *Advanced Research and Global Observation Satellite* (ARGOS). The HITS instrument observes the Doppler-shifted H Lyman-α emissions from proton precipitation with 1.5 Å resolution. The high spectral resolution of these measurements allows the auroral Lyman-α emissions to be separated from the intense geocoronal background. The measured proton aurora Doppler spectra are modeled using a Monte Carlo simulation of proton flux transport. The forward modeling performed with this code allows us to infer the characteristic energies of the incident protons from the measured Lyman-α Doppler spectra. The inferred characteristics of dayside versus nightside proton precipitation are compared and used to identify the magnetospheric regions from which the particles likely originated.

INDEX TERMS: 0358 Atmospheric Composition and Structure: Thermosphere—energy deposition; 2407 Ionosphere: Auroral ionosphere (2704); 2427 Ionosphere: Ionosphere/atmosphere interactions (0335); 2431 Ionosphere: Ionosphere/magnetosphere interactions (2736); 2455 Ionosphere: Particle precipitation.

1. Introduction

[2] Energetic protons originating from the ring current, radiation belts, and the plasma sheet precipitate into the upper atmosphere with some distribution in pitch angle and energy. The incident protons undergo collisions and experience charge exchange reactions with atmospheric constituents. Upon capturing an electron in a charge exchange interaction, a precipitating proton will propagate as an energetic hydrogen atom that preserves the velocity and direction of the original proton. If the hydrogen atom is in an electronically excited state, deexcitation may occur through photon emission. These emissions will be (red-) blue-shifted as it moves (away) toward an observer. Spectroscopic measurement of these Doppler shifts therefore provides a means of inferring precipitating proton energies, as was demonstrated by the pioneering work of *Vegard* [1939] and *Meinel* [1951] from ground-based measurements of H Balmer lines.

[3] Far-ultraviolet (FUV) measurements of H Lyman-α emissions from satellite-borne instruments have extended our capabilities for remote sensing of proton precipitation with greater spatial coverage and the ability to make observations under sunlit conditions in the dayside auroral regions. Recent efforts to better understand the synoptic structure of the proton aurora have been driven by the availability of global images of Doppler-shifted H Lyman-α emissions obtained by the IMAGE/SI-12 instrument [*Mende et al*., 2000, 2001]. To complement these global observations, high resolution spectral measurements of proton aurora with large spatial coverage are essential. Such data are obtained by the High Resolution Ionospheric and Thermospheric Spectrograph (HITS) aboard the *Advanced Research and Global Observation Satellite* (*ARGOS*) which provides detailed FUV observations of both the airglow and aurora. The HITS instrument is a *f*/5.4 1-meter Rowland circle spectrograph with a 100 Å selectable passband within the 500-1700 Å range. Individual HITS spectra have a time resolution of 1-second although these are typically averaged over longer time periods to improve the counting statistics. Over a 60-second interval HITS scans across approximately 200 km along the satellite track. The HITS field of view spans about 230 km in the cross track direction. The HITS observations offer two key advantages for proton aurora studies:

[4] (1) The spectral resolution of HITS achieved on orbit is about 1.5 Å (full-width, half-maximum). This is sufficient to separate the emissions from the geocorona at the Lyman-α rest wavelength and the Doppler-shifted Lyman-α emissions arising from proton precipitation. The inability to isolate these two Lyman-α components was a significant impediment toward detailed analyses of proton aurora spectra in previous studies.

[5] (2) The HITS proton aurora measurements from the ARGOS spacecraft are available in both dayside and nightside regions in both northern and southern hemispheres. The ARGOS spacecraft is in a 98.7° inclination, sun-synchronous 0230/1430 MLT polar orbit at 850 km altitude. While HITS is usually a limb-scanning instrument, the observations shown in this study are taken when HITS was set in a fixed viewing orientation wherein the angle between the HITS look vector and the spacecraft nadir vector is about 60°.

[6] The purpose of this report is to present the initial results from our study of high resolution spectral observations of proton aurora. The characteristics of proton aurora observed in the dayside auroral zone are contrasted with those seen in the nightside. The interpretation of the HITS proton aurora observations is aided with the use of a Monte Carlo model of proton and hydrogen transport and their interactions with the neutral atmosphere.

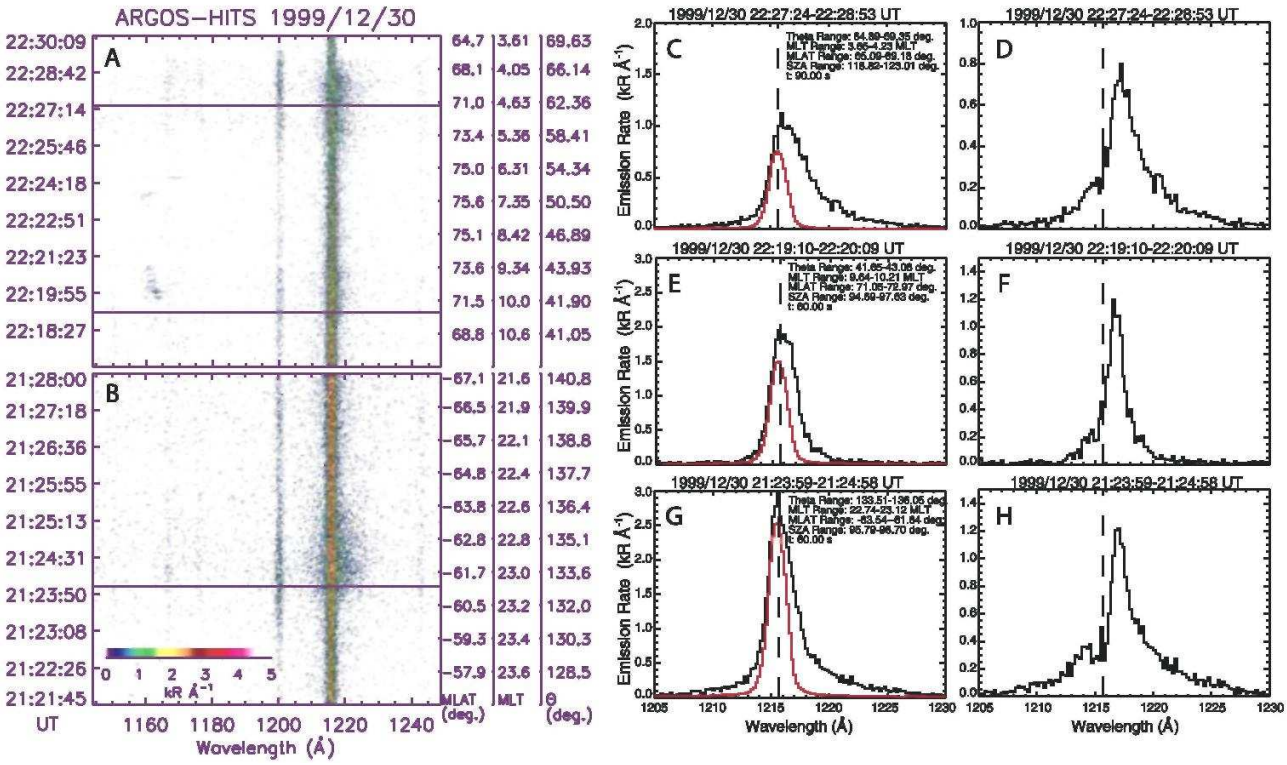

Figure 1. *HITS FUV auroral spectra in the northern (A) and southern (B) hemispheres. Panels C, E, and G show representative auroral spectra (black curves) and the estimated geocoronal Lyman-α contribution to the total line profile (red curves). Panels D, F, and H show the proton aurora Doppler spectra following subtraction of the geocoronal component. The vertical dashed lines in panels C-H denote the Lyman-α rest wavelength.*

2. HITS Observations

[7] HITS spectra obtained during the recovery phase of a substorm (AE ≥ 250 nT, Kp = 5^+) on December 30, 1999 are shown in Figure 1. The left-most panels show HITS auroral spectra in the northern (Figure 1A) and southern (Figure 1B) hemispheres. The wavelength scale (Å) and universal time are shown along each abscissa and ordinate respectively. The Apex magnetic latitude (MLAT) and magnetic local time (MLT) [*Richmond,* 1995] of the observations are shown along the secondary y-axes. Also shown is θ, the angle between the HITS look vector and the local IGRF magnetic field. The spectral emission rates are color coded in units of kiloRayleighs per Angstrom (kR $Å^{-1}$).

[8] The H Lyman-α emissions are the most prominent feature in these HITS spectra. Two components of this emission can be distinguished here: the ubiquitous geocoronal Lyman-α airglow at the rest wavelength (1215.67 Å) and Doppler-shifted Lyman-α emissions arising from precipitating protons. The latter appear as enhanced

emissions in the wings of the Lyman-α line within a narrow band of latitudes. In the southern hemisphere proton aurora are observed in the pre-midnight sector (2300 MLT) between -61° and -64° MLAT (Figure 1B). During the pass over the northern polar cap HITS observes proton aurora emissions in both the dayside (1000 MLT) and nightside (0400-0500 MLT) auroral zones (Figure 1A).

[9] Another important feature in the HITS dayglow and auroral spectra shown in Figure 1 is the NI 1200 Å triplet. Since the 1200 Å emission arises in part from electron impact excitation, it serves as a useful indicator of the electron aurora's location relative to the proton aurora. Additional weak spectral features with emission rates less than 50 R Å are present in Figures 1A and 1B, including the NI 1167 Å, 1176 Å, 1243 Å, and OI 1172 Å emission lines.

[10] In order to extract the Doppler-shifted Lyman-α proton aurora emissions from the HITS spectra it is necessary to first remove the geocoronal Lyman-α background. We measure the peak emission rate of the geocoronal Lyman-α line as a function of solar zenith angle outside the auroral regions where there are no contributions from proton aurora. This variation is modeled using a cosine squared function given in equation (1) where Φ_{SZA} is the solar zenith angle and $A_{0,1,2}$ are the fit parameters.

$$I = A_0 \cos^2 (A_1 \Phi_{SZA}) + A_2 \qquad (1)$$

An example of the geocoronal Lyman-α peak intensity versus solar zenith angle and the model fit using equation (1) is shown in Figure 2. Once the model is fit to the data, the expected geocoronal Lyman-α peak intensity at the auroral location of interest is computed using the fit parameters. The geocoronal background Lyman-α line shape is formed by convolving a delta function valued at the modeled peak intensity at the auroral location with the HITS line spread function. The resulting geocoronal Lyman-α line is then subtracted from the HITS spectra to yield the Doppler profile of the proton aurora emissions.

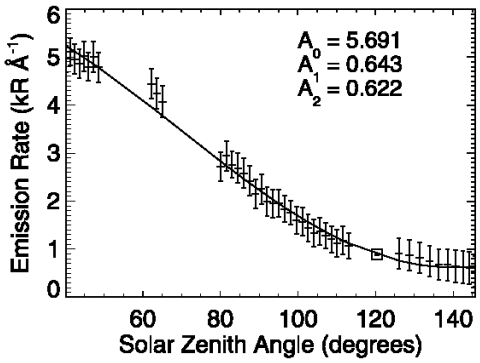

Figure 2. *Geocoronal Lyman-α peak intensity versus solar zenith angle. The model fit to the data using equation (1) is shown by the solid line. The data point near the solar zenith angle of 120° corresponds to the proton aurora location and shows the expected geocoronal Lyman-α peak intensity there based on the model fit.*

[11] Three examples of proton aurora spectra are given in Figures 1C, 1E, and 1G at the times indicated by the horizontal lines in Figures 1A and 1B. The auroral spectra (shown in black) are averaged over the amount of time, t, shown in each plot to improve the counting statistics. The red curve in each plot shows the modeled Lyman-α line used in subtracting the geocoronal background from the auroral spectra. The proton aurora Doppler spectra following geocoronal background subtraction are shown in Figures 1D, 1F, and 1H. We quantify these profiles by defining characteristic widths for the red and blue wings of the Doppler spectra as follows:

$$\Delta\lambda_{Red} = \frac{\int_{\lambda_{Ly\alpha}}^{\lambda_{max}} \lambda I(\lambda) d\lambda}{\int_{\lambda_{Ly\alpha}}^{\lambda_{max}} I(\lambda) d\lambda} - \lambda_{Ly\alpha} \; ; \; \Delta\lambda_{Blue} = \lambda_{Ly\alpha} - \frac{\int_{\lambda_{min}}^{\lambda_{Ly\alpha}} \lambda I(\lambda) d\lambda}{\int_{\lambda_{min}}^{\lambda_{Ly\alpha}} I(\lambda) d\lambda}$$

Here $\lambda_{Ly\alpha}$ is the H Lyman-α rest wavelength and 1(λ) is the spectral emission rate at each observed

wavelength.λ_{min} and λ_{max} are the lower and upper limits of integration for the blue and red widths. These are set to λ_{min} = 1210.0 Å and λ_{max}= 1230.0 Å, corresponding to H/H^+ energies of 10.3 keV (upward propagating) and 64.4 keV (downward propagating) respectively. The characteristic red and blue widths indicate the hardness of the H/H^+ distributions giving rise to the measured emissions: larger spectral widths correspond to more energetic H/H^+ populations.

[12] During the orbit shown in Figure 1A, dayside proton aurora is observed between 22:19-22:21 UT in the high latitude (70-73° MLAT) pre-noon sector (1000 MLT). Subtracting the modeled geocoronal Lyman-α line yields the dayside proton aurora Doppler spectrum shown in Figure 1F. The red-shifted wing of this dayside proton aurora spectrum peaks at 1216.6 Å and is narrow with a characteristic width of 2.1 Å. The faint blue wing of this dayside proton Doppler spectrum indicates the presence of a weak backscattered H/H^+ component. The emission rates in the blue wing of the dayside proton spectrum are less than 150 Rayleighs and the characteristic width is 1.3 Å.

[13] Doppler-shifted H/H^+ emissions in the nightside proton aurora extend beyond 1225.0 Å which is indicative of higher energy proton precipitation. Near the equatorward region of the northern auroral zone (65-69° MLAT), between 22:27:24-22:28:53 UT, HITS observes a broad red wing in the proton aurora spectrum with a characteristic width of 3.4 Å (Figures 1C and 1D). The peak in the Doppler-shifted proton aurora spectra appears at 1217.2 Å. A stronger blue wing is seen here than on the dayside aurora with a characteristic blue width of 1.8 Å. The proton aurora observed by HITS between 21:24-21:25 UT in the southern hemsiphere, pre-midnight sector is similar to that measured in the post-midnight, northern hemisphere (Figures 1G and 1H). Here, the peak in the Doppler profile occurs at 1217.0 Å and the characteristic red and blue widths are 3.5 Å and 2.1 Å respectively (Figures 1G and 1H).

3. Model Comparison

[14] In Figure 3 the HITS proton aurora spectra (black curves) are compared to synthetic Doppler-shifted Lyman-α line profiles (gray curves) produced by a Monte Carlo simulation of proton and hydrogen transport. Protons with some distribution in pitch angle and energy (i.e. Maxwel-lian, kappa, mono-energetic) are input into a MSIS-90 model atmosphere [*Hedin,* 1991] and their transport through the neutral atmosphere is described by solving a set of coupled Boltzmann equations. The model includes elastic and inelastic collisions, ionization, and charge exchange. Further details of the model are described by *Gérard et al.* [2000]. The excitation of Lyman-α emissions is computed and a synthetic Lyman-α Doppler profile matching the HITS viewing geometry and convolved with the HITS line spread function is produced. The input parameters of the forward model are varied until the χ^2 statistic is minimized when comparing the predicted and observed proton aurora spectra. In each case, the proton aurora line profile produced by the model is added to the geocoronal Lyman-α line (from Figures 1C, 1E, and 1G) in order to reproduce the original HITS spectral measurement. For this study we assume an isotropic pitch angle distribution for the protons input into the model. The incident protons are given a kappa energy distribution (κ, = 3.5) and the proton characteristic energies (E_0) are varied between 100 eV and 25 keV.

[15] For the narrowly-peaked dayside proton spectrum the observed Doppler profile is best fit by an input proton distribution with a characteristic energy near 1 keV (Figure 3, top panel). The model reproduces the peak in the auroral spectrum well, and we see good agreement in the predicted and observed red wing emissions longward of 1217 Å. The model predicts a larger backscattered H/H^+ component than the observed spectra shows, since the blue wing of the modeled spectrum is more intense than that measured.

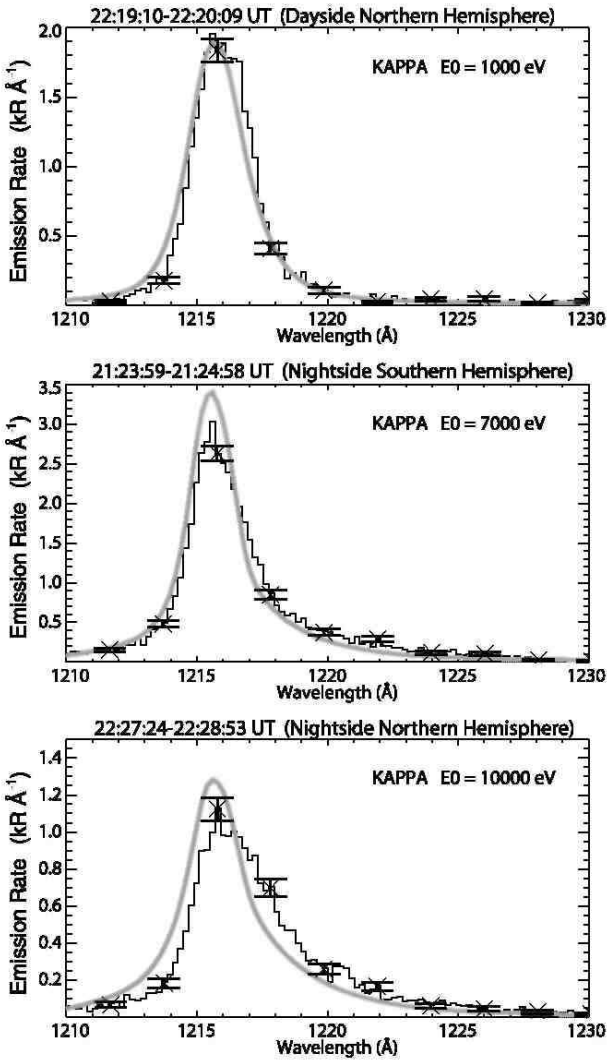

Figure 3. *Monte Carlo model fits to proton aurora Doppler spectra observed by HITS in the dayside northern hemisphere (top), nightside southern hemisphere (middle), and the nightside northern hemisphere (bottom).*

[16] The proton aurora spectrum measured by HITS in the nightside southern hemisphere is best matched by precipitating protons with a characteristic energy of 7 keV (Figure 3, middle panel). The model closely reproduces the observed blue wing of the proton spectrum, indicating that the fraction of backscattered H/H^+ from the input proton beam is estimated well. The model overestimates the peak in the auroral spectrum by 13% and underestimates the intensity of the red wing relative to the observations. The bottom panel of Figure 3 shows the comparison of the spectrum measured by HITS in the northern, nightside auroral zone and the modeled Doppler profile arising from proton precipitation with a characteristic energy of 10 keV. While the general shape of the modeled proton aurora Doppler profile is similar to that of the observations, the HITS spectrum appears red shifted by about 1 Å relative to the model prediction. The peak of the modeled Lyman-α line profile is also about 20% more intense than the observed spectrum.

4. Discussion and Conclusions

[17] The characteristics of the precipitating protons inferred from the HITS observations allude to their likely origins in the magnetosphere. With a narrow Doppler spectrum and an inferred characteristic energy near 1 keV, the precipitating protons observed by HITS in the dayside aurora near the northern polar cap probably represent a magneto sheath-like population originating from either the mantle or low-latitude boundary layer (LLBL). The observed dayside proton aurora is not likely to be associated with H/H^+ precipitation from the cusp since the HITS measurement was taken in the pre-noon sector during a period when the B_y component of the interplanetary magnetic field (IMF) was strongly positive (not shown). Previous studies have shown that the cusp is located in the post-noon sector when the IMF B_y component is positive [*Frey et al.,* 2002, for example].

The nightside proton aurora seen by HITS is consistent with H/H^+ precipitation from the plasma sheet, given the relatively broad Doppler profiles and inferred characteristic energies in the 7-10 keV range.

[18] The synthetic proton aurora spectra produced by the Monte Carlo H/H^+ transport model agreed well with the observed Doppler profiles in two of the three cases shown (Figure 3). In the third case, the predicted and observed proton spectra had similar profiles but the measured spectrum appeared red-shifted relative to the model spectrum. One explanation for this is that the incident proton beam is not isotropic as we have assumed in the model. If the pitch angle distribution of the incident protons is more field-aligned, the fraction of incident particles that continue to be scattered downward to produce red-shifted emissions increases relative to the fraction that can undergo either magnetic mirroring or sufficient scattering to change their pitch angles beyond 90°. This produces Doppler spectra with peaks at longer red-shifted wavelengths and with diminished blue wings. Figure 4 of *Gérard et al.* [2000] illustrates this behavior.

[19] One situation in which the above scenario would be likely is if the nightside northern hemisphere proton spectrum shown in Figures 1C and 3 was obtained equatorward of the proton isotropy boundary (IB) *[Sergeev et al,* 1983] in a low-latitude proton precipitation (LLPP) region [*Gvozdevsky et al*., 1997, and references therein]. Normally the flux of trapped protons (J_t) and the flux of precipitating protons (J_p) are comparable poleward of the proton isotropy boundary (isotropic proton flux distribution). Equatorward of the isotropy boundary J_t remains high while J_p usually drops rapidly. However during LLPP events there is an enhanced flux of precipitating protons equatorward of the isotropic boundary caused by the partial filling of the loss cone by a moderate amount of pitch angle scattering. The proton pitch angle distributions in LLPP regions are usually anisotropic ($J_p/J_t < 1$). LLPP typically occur following substorms, as is the case for our observations.

[20] Further studies of proton aurora using HITS observations will include establishing a quantitative relationship between the observed red and blue widths of the Doppler profiles ($\Delta\lambda_{Red}$, $\Delta\lambda_{Blue}$) and the characteristic energies of the incident protons inferred by the Monte Carlo proton transport model. Coordinated observations between HITS and global images from the IMAGE/SI-12 instrument will also enrich our understanding of the large scale structure and dynamics of proton aurora.

[21]Acknowledgments

This work was performed while D. Chua held a National Research Council Research Associateship Award at the Naval Research Laboratory. J.-C. Gérard is supported by the Belgian National Fund for Scientific Research (FNRS) and V. Coumans by a fellowship from the Belgian National Fund for Research in Industry and Agriculture (FRIA). This work was partly funded by the PRODEX program of the European Space Agency (ESA) and the Belgian Fund for Collective Fundamental Research (FRFC).

References

Frey, H. U., S. B. Mende, T. J. Immel, S. A. Fuselier, E. S. Claflin, J.-C. Gérard, and B. Hubert, Proton aurora in the cusp, *J. Geophys. Res*., *107*(A7), 1091, doi: 10.1029/2001JA900161, 2002.

Gérard, J.-C, B. Hubert, D. V. Bisikalo, and V. I. Shematovich, A model of the Lyman-α profile in the proton aurora, *J. Geophys. Res*., *105*, 15,795, 2000.

Gvozdevsky, B. B., V. A. Sergeev, and K. Mursula, Long lasting energetic proton precipitation in the inner magnetosphere after substorms, *J. Geophys. Res*., *102*, 24,333, 1997.

Hedin, A. E., Extension of the MSIS thermosphere model into the middle and lower atmosphere, *J. Geophys. Res*., *96*, 1159, 1991.

Lummerzheim, D., and M. Galand, The profile of the hydrogen Hβ emission line in proton aurora, *J. Geophys. Res*., *106*, 23, 2001.

Meinel, A. B., Doppler shifted auroral hydrogen emission, *Astrophys. J*., *113*, 50, 1951.

Mende, S. B., et al., Far ultraviolet imaging from the IMAGE spacecraft: 3. Spectral imaging of Lyman alpha and OI 135.6 nm, *Space Sci. Rev*., *91*, 287, 2000.

Richmond, A. D., Ionospheric electrodynamics using magnetic apex coordinates, *J. Geomag. Geoelectr*., *47*, 191, 1995.

Sergeev, V. A., E. M. Sazhina, N. A. Tsyganenko, J. Å. Lundblad, and F. Soraas, Pitch angle scattering of energetic protons in the

magnetotail current sheet as the dominant source of their isotropic precipitation into the nightside ionosphere, *Planet. Spa. Sci., 31*, 1147, 1983.

Vegard, L., Hydrogen showers in the auroral region, *Nature*, *144*, 1089, 1939.